

# Clinical and experimental study on regional administration of phosphorus 32 glass microspheres in treating hepatic carcinoma

LIU Lu, JIANG Zao, TENG Gao-Jun, SONG Ji-Zhi, ZHANG Dong-Sheng, GUO Qing-Ming, FANG Wen, HE Shi-Cheng, GUO Jin-He

**Subject headings** liver neoplasms/therapy; phosphorus-32 glass microspheres ( $^{32}\text{P-GMS}$ );  $^{31}\text{P-GMS}$ ; interventional therapy

## Abstract

**AIM** To study the therapeutical effectiveness, dosage range and toxic adverse effects of domestic phosphorus 32 glass microsphere and evaluate its clinical significance.

**METHODS** I. Fifty-two BALB/c tumor bearing male nude mice were allocated into treatment group ( $n = 38$ ) and control group ( $n = 14$ ). In the former group different doses of  $^{32}\text{P-GMS}$  were injected into the tumor mass, while in the latter  $^{31}\text{P-GMS}$  or no treatment was given. The experimental animals were sacrificed in batches, and then the tumors and their nearby tissues were examined by light and electron microscopy. II. Through selective catheterization of hepatic artery,  $^{32}\text{P-GMS}$  was infused to 5 healthy domestic pigs in a dosage equivalent to the therapeutic dose for human being, and  $^{31}\text{P-GMS}$  was infused to another 5 healthy domestic pigs. Two pigs infused with contrast medium served as whole course blank controls. One pig from each group was surrendered to euthanasia at week 1, 4, 8 and 16 respectively. The ultrastructural histopathological changes in liver tissues taken from different sites were evaluated *semiquantitatively*. III. One hundred and twenty-seven times of  $^{32}\text{P-GMS}$  intrahepatic artery interventional therapies were performed on 93

patients with hepatic carcinoma, including 79 cases of primary hepatic carcinoma and 14 cases of secondary hepatic carcinoma.  $^{32}\text{P-GMS}$  ( $n = 30$ ), and group B,  $^{32}\text{P-GMS}$  and half-dose of trans-hepatic artery embolization (TAE) ( $n = 49$ ), and 18 patients with HCC by TAE only as control group C. Fourteen patients with secondary hepatic carcinoma were treated in the same way as group B or C.

**RESULTS** I. Comparing with the control group, the treatment group of tumor bearing nude mice attained the tumor inhibition rates of 59.7%-93.7% ( $F = 579.62$ ,  $P < 0.01$ ) at 14d. At an absorbed dose of 7320Gy, the tumor cells were completely destroyed. When the absorbed doses ranged from 1830Gy to 3660Gy, most of the tumor cells showed the evidences of injury or necrosis, but there appeared some well-differentiated tumor cells and enhanced effect of the autoimmunocytes. At an absorbed dose of 366Gy or less, some tumor cells still remained active proliferative ability. The definite anticancer effect appeared as early as 3d after intratumoral injection of  $^{32}\text{P-GMS}$ . II. The cumulative amount of  $^{32}\text{P-GMS}$  in the target tissue after trans-hepatic artery instillation attained more than 90% of the total dose administered. Semiquantitative analysis of ultrastructural morphology in the experimental group showed no statistical difference between the nuclear abnormality ( $n_{\text{abn}}$ ) and mitochondrial variability ( $M_{\text{var}}$ ) at week 1 or 2, but revealed prominent difference ( $\chi^2 = 6.70-9.68$ ,  $P < 0.01$ ,  $\chi^2 = 65.09-115.09$ ,  $P < 0.001$ ) as compared with those in the other groups. In the experimental group the  $n_{\text{abn}}$  in tissues showed no significant difference between week 8 and week 16. no apparent changes were found in the stomach, spleen, kidney and lung tissues of the experimental pigs. III. The therapeutical results of HCC patients in group A were closely approximated to those of group C, no hematological toxic side effects were noted, and the systemic reaction was mild. In some patients 2 mos-3 mos after treatment some secondary

Experimental Center of Modern Medical Sciences, Nanjing Railway Medical College, Nanjing 210009, Jiangsu Province, China  
LIU Lu, M.D. female, born in 1946-10-17 in Jinan, Shandong Province, Han nationality, graduated from Nanjing Railway Medical College in 1970 and is now an Associate Professor, majoring in nuclear medicine and having more than 50 papers published at home and abroad.

Supported by the Science and Technology Commission of Jiangsu Province, No. BJ93077. Sponsored by Project No. 863 of National High-Tech Research and Development Program, No. 715-002-0200.  
**Correspondence to:** LIU Lu, Experimental Center of Modern Medical Sciences, Nanjing Railway Medical College, Nanjing 210009, China  
Tel. +86-25-3301508 Ext. 2708, Fax +86-25-3426368  
Email.xue-c@263.net  
Received 1999-07-14

**foci appeared around the periphery of the primary lesion. In general better effectiveness was obtained in patients with small lesion. After analyzing by RIDIT method, the therapeutic result in group B was significantly better than that in group C, and secondary foci around the original lesion were rarely seen at 3mos after treatment. In group C the collateral circulation was reestablished along the periphery of primary foci and the secondary foci appeared more frequently, and were required to undergo several courses of treatment. In group B, 4 cases of HCC were treated surgically as their mass decreased in size after <sup>32</sup>P-GMS treatment. Resected specimens showed that the tumor was encapsulated by fibrotic tissue and most of the tumor cells necrosed. The 3-year survival rates were 43.3%-51.0% after A and B regimen treatment. In 14 cases of secondary HCC, the foci were well controled within one year after-treatment.**

**CONCLUSION When the experimental model of implanted human liver cancer cells received <sup>32</sup>P-GMS of 1830Gy-3660Gy, it produced excellent anticancer effect without any injury to the normal neighboring tissues and the prominent anticancer effect was shown within 3d after intratumoral injection. Intrahepatic arterial administration of <sup>32</sup>P-GMS at the macrocosmic absorbed dosage less than 190 Gy/dose exerted reversible sub-lethal injury to domestic pig liver tissues. It took more than 8 weeks to repair the injured liver tissue and restore its function. <sup>32</sup>P-GMS trans-hepatic artery embolization is an effective and safe regimen in treating hepatic carcinoma.**

## INTRODUCTION

Trans-hepatic artery embolization (TAE)<sup>[1]</sup> is the main regimen for treating unresectable hepatic carcinoma (HCC). The experimental investigation using microsphere carriers such as colloidal microsphere, artificial cell membrane-liposome etc, in treating malignant tumors had been carried out for more than a decade with advanced development<sup>[2]</sup>. The microspheres mainly conjugated with anticancer drugs released slowly into the cancer tissue. Up to now, a novel anticancer microsphere preparation has been evolved, i.e. incorporation of radionuclide (<sup>32</sup>P or <sup>90</sup>Y) to the glass microspheres forming a nontoxic, undegradable radioactive radiation source through

regional medication, which aroused the interest and notice of investigators in this field<sup>[3-5]</sup>.

We report the results of evaluating the pharmacology, toxicology and clinical effect of <sup>32</sup>P-phosphorus-glass microspheres (<sup>32</sup>P-GMS) in three parts. I. By using human liver cancer cell bearing nude mouse model to explore the experimental anti cancer effect of intratumoral injection of <sup>32</sup>P-GMS and investigate the appropriate dose range, time course and the influence on the neighboring tissues. II. By administrating <sup>32</sup>P-GMS to the whole liver or certain liver lobes of domestic pig model and observing the local irradiative reaction and systemic toxic effect on the normal liver tissue to provide the experimental basis for determining the appropriate tolerable dosage and treatment course of <sup>32</sup>P-GMS internal irradiation in normal human liver tissues. III. From 1996 to 1998, 93 patients with liver cancer received 127 times of interventional <sup>32</sup>P-GMS internal irradiation.

## MATERIALS AND METHODS

### *Medicaments*

By activation of standardized glass microspheres with nonradioactive <sup>31</sup>P (<sup>31</sup>P-GMS, cold sphere) through nuclear-chemical reaction [<sup>31</sup>P (n,γ)<sup>32</sup>P] transformed into radioactive <sup>32</sup>P glass microsphere (provided by nuclear Power Research Institute of China, nPIC)<sup>[6]</sup>, having the properties as follows: diameter of glass sphere 46 μm-76 μm, radioactive nuclide purity >99%, radioactivity per unit 550 MBq·g<sup>-1</sup> 3700 MBq·g<sup>-1</sup> (15 mCi·g<sup>-1</sup>-100 mCi·g<sup>-1</sup>), <sup>32</sup>P elution rate <0.1% within 30 days; <sup>32</sup>P physical half-life 1428 days, average β ray energy per disintegration: 0.695 MeV (maximum energy 1.711 MeV); and soft tissue penetration distance, max. 8.0 mm, averaging 3.2 mm. <sup>32</sup>P-GMS suspension was prepared by mixing <sup>32</sup>P-GMS with super-liquidized iodized oil or 50% glucose solution to the concentration of 100 mg·mL<sup>-1</sup> on oscillator.

### *Dosimetry*

Loevinger's formula<sup>[7]</sup> for calculating the absorbed dose of β emitter radionuclide:

$$D_{\beta\infty} = 73.8E_{\beta}C_0T_{\text{eff}}$$

where  $D_{\beta\infty}$  the total absorbed beta particle dose (cGy),  $E_{\beta}$ , the average beta ray energy per disintegration (MeV),  $C_0$ , the initial tissue concentration of radioactivity (mCi/kg) and  $T_{\text{eff}}$ , the effective half-life (days).

Based on the pharmacokinetic characteristics of regional administration of <sup>32</sup>P-GMS and the related parameters, the following formulae were established<sup>[8]</sup>:

$$D \text{ (cGy)} = 20A \text{ (MBq)} \cdot m \text{ (kg)}^{-1}$$

$$D \text{ (cGy)} = 732A \text{ (mCi)} \cdot m \text{ (kg)}^{-1}$$

where A: the cumulative activity of radioactive nuclide, D: the total dose of absorbed  $\beta$  particles in tissue, m: the tissue weight.

### Animal experiment

**Human liver cancer cell-bearing nude mouse model and anti-cancer effect of  $^{32}\text{P}$ -GMS** Human liver cancer cell line subset (H-CS)<sup>[9]</sup> with higher oncogenicity and liability of metastasis was implanted into the dorsal subcutaneous tissue of 52BALB/c nu/nu nude mice (male, body weight 16.8 g-21.3 g, mean 19.2 g, aged 4 weeks, derived from Shanghai Experimental Animal Center, Chinese Academy of Sciences) at the dosage of 0.1 mL-0.2 mL ( $1 \times 10^7$  tumor cells for each animal).

Experiment 1. Forty tumor-bearing nude mice with the tumor mass diameter of 0.7 cm-1.0 cm, different doses of  $^{32}\text{P}$ -GMS were injected to the mass center of 32 nude mice (subgroup 1-V) in the treatment group and non-radioactive  $^{31}\text{P}$ -GMS to mass center of 8 nude mice as the control subgroup. The animals were sacrificed on the 14th day.

Experiment 2. Twelve tumor-bearing nude mice with matched tumor size were equally allocated into treatment and control group, and  $^{32}\text{P}$ -GMS 3.7 MBq were injected to the tumor mass at points with 0.8 cm apart from each other, the total dosage being 7.4 MBq-14.8 MBq, varied with the size of tumor. no treatment was given to the control animals. The mice in the treatment group were sacrificed in batches on day 3, 6, 13, 20, and 28 after medication and the same was done for those in control group. The tumor masses were disposed similar to Experiment 1. One mouse in both treatment and control groups died on day 19 and 22 spontaneously without any difference from the survivals in appearance. All of the tumor specimens were submitted to gross inspection, light and electron microscopy to observe the morphological and ultrastructural changes and then calculate the tumor inhibition rate. Tumor inhibition rate (at the time of execution) = (tumor weight of control-tumor weight of treatment group) / tumor weight of control group  $\times 100\%$ .

### Experimental study on the toxicology of $^{32}\text{P}$ -GMS

Twelve domestic pigs (6 males, 6 females) with average body weight of 23.4 kg, were randomly divided into 3 groups: warm sphere group,  $^{32}\text{P}$ -GMS ( $n = 5$ ), cold sphere group  $^{31}\text{P}$ -GMS ( $n = 5$ ) and whole course blank control group ( $n = 2$ ). Under generalized anesthesia the catheter was inserted through femoral artery to the hepatic artery of the experimental animal. To the warm sphere group  $^{32}\text{P}$ -GMS was administered at a dose equivalent to that of man,  $^{31}\text{P}$ -GMS administered to the cold

sphere group and roentgenographic contrast medium to the blank control group. For the pigs with  $^{32}\text{P}$ -GMS, the distribution of nuclide radioactivity was studied by SPECT. The radioactivity count rate was recorded on the body surface of hepatic, pulmonary and splenic regions of pigs for 14 consecutive days. One pig a time was surrendered to euthanasia on week 1, 2, 4, 8 and 16. The animal liver was dissected and weighed as soon as possible. From different sites of liver 8 tissue specimens were taken for light and electron microscopy. And at the same time, the major organs suspected to be involved such as lung, spleen, stomach and kidney were sampled for light microscopy. At the corresponding time point, liver biopsies were performed on the rest surviving animals for light and electron microscopy.

Venous blood specimens were taken for routine blood count, estimation of liver and renal function and for dynamic study of liver fibrosis markers, such as hyaluronic acid (HA), human procollagen III (hPCIII), collagen IV(C-IV), laminin (LN) and glycocholate (CG) by radioimmunoassay. The specimens prepared routinely were studied under H-600 electron microscopy at 8 000 folds magnification, to observe the ultrastructure and analyze morphometrically. A total of 100 hepatocyte nuclei and 100 mitochondria were observed in each sample group, and the nuclear abnormality ( $N_{\text{abn}}$ ) and mitochondrial variability ( $M_{\text{var}}$ ) were calculated respectively. The characteristics of abnormal nuclei were: nuclei irregular and deformed in shape; abnormal nuclear membrane, distension of the perinuclear gap; abnormal chromatin with peripheral condensation, and increase in intranuclear inclusion bodies with giant nucleolus. The abnormal mitochondria were characterized by swelling with disrupted external membrane and decrease in cristae; shrunken mitochondria, deep staining of ground matrix with decreased granules but with some vacuoles. The rates of abnormal nucleus and mitochondria variation were the percentage calculated from the number of abnormal or variation per total number of nuclei observed.

### Preliminary clinical application of $^{32}\text{P}$ -GMS in treating hepatic carcinoma

**Clinical materials** Seventy-nine cases of primary hepatocellular carcinoma, male 67 and female 12 with average age of 52 years (32 years-77 years). The diagnosis was based on the evidence afforded from the results of B-mode sonography, computed tomography or angiogram and blood AFP  $> 400 \mu\text{g/L}$ . In some cases with negative AFP, their pathological and cytological evidence settled the diagnostic problem. The clinical types in 79 cases of HCC were single massive types (52 cases, left lobe 3, right lobe 49); multi-nodular type (24 cases); and

diffuse type (3 cases). According to Child's classification of liver function, 25 were of grade A, 40 grade B and 14 grade C. The average diameter of tumor mass was 8 cm (3 cm-15 cm), 62 cases (78.5%) showed positive hepatitis B antigen, 52 cases (65.8%) were complicated with cirrhosis, 4 cases (5.1%) portal vein embolization, 6 (7.6%) pulmonary metastasis, 7 (8.9%) peritoneal lymph node metastasis and 8 (10.1%) had family histories of gastrointestinal tumors. In 14 cases of secondary hepatic carcinoma, 6 were primary colonic tumors, 5 gastric, 1 pulmonary and 2 esophageal cancers.

**Treatment regimen and grouping** Superselective catheterization was performed by Seldinger's procedure to the distal end of hepatic artery proper for 127 times in 93 cases of hepatic carcinoma. No hepatic A-V fistula was found in all of the cases as confirmed by DSA, then the <sup>32</sup>P-GMS suspension prepared by occlusion of super-liquidized iodized oil 4 mL-10 mL and <sup>32</sup>P-GMS with calculated tumor tissue absorbed dose of 50Gy -100Gy and activity range from 370 MBq-470 MBq was instilled. HCC patients were allocated randomly into 3 groups. Group A: <sup>32</sup>P-GMS internal irradiation embolization therapy (30 cases); Group B: <sup>32</sup>P-GMS and half dose TAE [Adriamycin (Adr) 30 mg/m<sup>2</sup>+cis-diammine dichloroplatinum (CDDP) 50 mg/m<sup>2</sup>+iodized oil] combined therapy (49 cases); Group C: TAE (18 cases). Fourteen cases of secondary hepatic carcinoma were treated by B and C regimen. After embolization the vasculature and tumors staining disappeared on DSA.

**Follow-up** Before treatment the average life quantity score was 65.5 (Karnofsky score)<sup>[10]</sup>. The results in liver and renal function, ECG, routine blood counts, blood AFP and CEA on day 10-14 after treatment were compared with the corresponding basal data. SPECT liver images were conducted in 20 cases before treatment. Distribution of nuclide radioactivity in chest and abdomen within 80 h after treatment was studied using bremsstrahlung lung conducted by SPECT. Plain film of liver region showed the foci of condensed iodized oil shadow within 5 days after treatment. B-mode sonogram, or computed tomogram or plain film of abdomen was taken at the scheduled time of follow-up.

**Evaluation of therapeutical results** According to the modified WHO<sup>[10]</sup> criteria for tumor therapy, the effectiveness of grades A, B and C was the product of two perpendicular diameters which were decreased >50%, 50%-25% and 25%-10%, respectively, while the product decreased <10% was defined as stable. When the product was increased, it meant ineffective.

### Statistical method

Chi-square test and RIDIT method were used for analyzing categorical data, *t* test and ANOVA were used for analyzing numerical data and survival rate was calculated by life-table method.

## RESULTS

### Changes in implanted human hepatic carcinoma

**Gross inspection (Figure 1)** The similar manifestation in Experiments I, II and controls was the rapid progressive growth of tumor mass, beginning from the dorsal injection points extended to the contralateral side, eventually distributed to the whole dorsa and buttocks. At the time of execution, the tumor mass presented nodular or lobular in shape with axial diameter of 2.3 cm - 4.0 cm, hard and firm in consistency on palpation with thin intact reddish covering epiderma without ulceration. After the covered epiderma was incised, there was plenty of blood vessels on the mass surface, bleeding readily, and the section showed light reddish in color, dense in consistency, rich in vessels, and sometimes with central necrosis and focal liquification. In the treatment group the growth of tumor mass was evidently inhibited, and the inhibiting rate was directly proportional to the dosage administered and time elapsed (Tables 1, 2). About 5 days after medication, the tumor mass began with ulceration, bleeding or petechia, liquification and cystic degeneration. These changes might result in increase in tumor size, but that was qualitatively different from the growth of tumor in control group. The tumor of subgroups I and II shrank with scars or cystic degeneration. The section of tumor showed grayish white color with poor vascularity. In subgroups III-IV, most of the implanted tumors presented with ulceration, bleeding, liquification and cystic degeneration, the section of tumor showed grayish white in color with poor vascularity, too. These changes had already appeared on 3 day after medication.

**Table 1** Nude mice in different absorbed dosage group the tumor weight (g) variance, SNK analysis and tumor inhibiting rate (14d)

Group	No. of Cases (n)	Tumor weight <sup>①</sup> ( $\bar{x}\pm s$ )	SNK <sup>②</sup>	Absorbed dose mean value (Gy)	Tumor inhibiting rate (%)	Necrosed tumor cell (%)
Control	8	6.25±0.39	A	-	-	4
I	6	0.40±0.10 <sup>a</sup>	B	7320	93.6	82
II	6	0.46±0.08 <sup>a</sup>	B	3660	92.5	78
III	8	0.94±0.10 <sup>a</sup>	C	1830	84.8	70
IV	6	2.17±0.26 <sup>a</sup>	D	366	65.3	47
V	6	2.43±0.33 <sup>a</sup>	E	183	59.7	40

①Variance analysis of the mean tumor weight of different doses and control group after square root correction,  $F = 579.62$ ,  $^aP < 0.01$ . ②Different or same alphabets denote with or without statistical significance of mean deviations between groups respectively.

**Table 2 Relationship between tumor inhibiting rate and execution time in tumor-bearing nude mice accepted  $^{32}\text{P}$ -GMS in absorbed dose of 366Gy**

Time of execution (d)	Weight of tumor (g) treatment group/control group	Tumor inhibiting rate (%)
3	1.5/2.3	34.8
6	1.7/3.2	46.9
13	2.1/5.9	64.4
20	1.6/6.7	76.1
28	1.0/6.8	85.3

**Light microscopy (Figure 2)** The tumor cells of control group were closely arranged in the form of trabeculae with large nuclei and prominent nucleoli. Some cells showed binuclei or giant nucleus and mitosis were readily found. Plenty of blood sinusoids and concentrated bile could be found between the intercellular space of tumor cells. Some of the tumor tissues showed fatty change or scattered focal necrosis. In the treatment group the microscopic manifestation varied with the different activities of the  $^{32}\text{P}$ -GMS administered. In the I and II subgroups the tumor cells were loosely arranged with widely distributed coagulation necrosis. Some nuclei showed prominent shrinking degeneration. In subgroup III the tumor cells were loosely arranged and separated by thick or thin bundles of vesiculo-fibro-connective tissue forming pseudoacini, and in the nest some nuclei were broken with deeply stained scant cytoplasm. The histological characters in subgroups IV and V were that the arrangement of tumor cells transformed from dense to loose with scattered spot necrosis, blood sinuses being not found. In loosely arranged tumor cells desmosomes were fewer than those in the closely arranged tumor cells, but the degenerated necrotic cells increased. The necrosis was mainly located at the center of tumor mass and scattered among the dispersed tumor cells. In this experiment, a tumor mass with largest dose of radiation showed metaplasia in the neighboring epidermal tissues.

**Electron microscopy (Figure 3)** In the control group, most of the tumor cells were poorly differentiated and rapidly multiplied, with the characteristics of irregular large nuclei with deep indentation, pseudo-inclusion body formation, large and prominent nucleoli, several peripherally aggregated, nucleoli with plenty of chromatin in it. In cytoplasm mainly free polyribosome presented, while mitochondria, glycogen and rough endoplasmic reticulum were scant. In the nearby interstitial tissue infiltrated tumor cells, degenerated lymphocytes, damaged fibroblasts,

loose collagen fiber, and many vesicular inclusion bodies in the nuclei were found. The tumor cells of subgroup I revealed necrotic injury, and in the severely injured cells the nuclei lysed, cell membrane disrupted and numerous debris were found. The injured tumor cells showed condensation of nuclear chromatin, peripheral aggregation of heterochromatin in pieces, damaged organelles in cytoplasm, disappearance of mitochondrial cristae and ribosomes, appearance of many vacuoles and lipid particles. In subgroup II, many tumor cells presented histological structures similar to those in subgroup I, but with many lysosomes and mimetic secretory granules. Some were differentiated tumor cells with the characters of round nucleus with small nucleolus, evenly distributed chromatin, mainly euchromatin, mitochondria and rough endoplasmic reticula in the cytoplasm, formation of microvilli at the interface of tumor cells. The capillaries between the moderately differentiated tumor cells had thickened or loosened basal membrane with local defects, and abundant fibroblast and collagen fibers could be found in the matrix. And there was a tendency of bile canal iculi formation somewhere in the matrix. The tumor cells in subgroup III showed different morphologic appearance, some damaged mildly and others severely, but some were moderately differentiated with plenty of cytoplasmic free polyribosomes. Plasma cells scattered among the tumor cells, and some lymphocytes protruded pseudopodia when contacted with the tumor cells, no abnormality was found in the dermal cells of adjacent skin. There were residual tumor cells showing active proliferation in subgroup IV, and some normal or degenerated lymphocytes, fibroblasts and collagen fibers presented in the interstitial tissue near the tumor. In subgroup V, the histological structure was manifested in various complicated forms, and the active multiplication of tumor cells were readily seen.

#### *Toxicological manifestation of liver tissue in domestic pigs*

**Absorbed dose of  $^{32}\text{P}$ -GMS** Liver tissue histological parameter of domestic pigs with intrahepatic arterial administration of  $^{32}\text{P}$ -GMS and the absorbed dose of internal radiation in liver lobe at the time of euthanasia were estimated (Table 3). By scanning the different body surface regions of experimental pigs, the macrocosmic radioactivity counts in the target organ might attain more than 90% of total dose of  $^{32}\text{P}$ -GMS given through the hepatic arterial catheterization. The effect of the dispersed radiation was also included in this rate.



**Figure 1** ①After intratumoral injection of  $^{32}\text{P}$ -GMS, SPECT revealed radioactive image condensed in the tumor but not in the non-target tissue. ②On the 14th day tumor in treatment group shrank prominently. ③Increased in size and plenty of blood supply in control group.

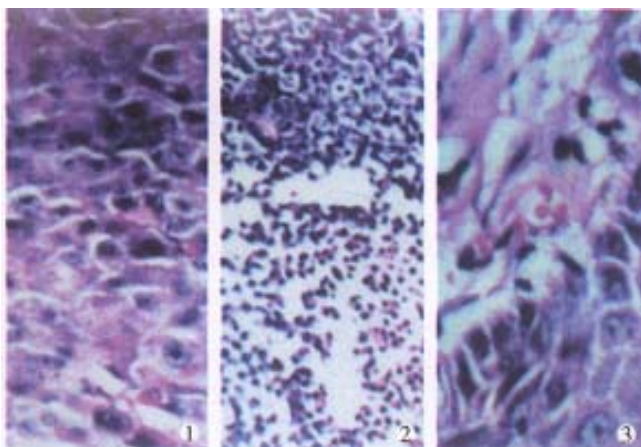


**Figure 2** On the 14th day, ①Control group tumor cells densely arranged and actively growing (HE $\times$ 100). ②Treatment group, tumor cells in coagulation necrosis (HE $\times$ 100). ③ Treatment group, radiation injury in neighboring epidermal tissue (HE $\times$ 200).

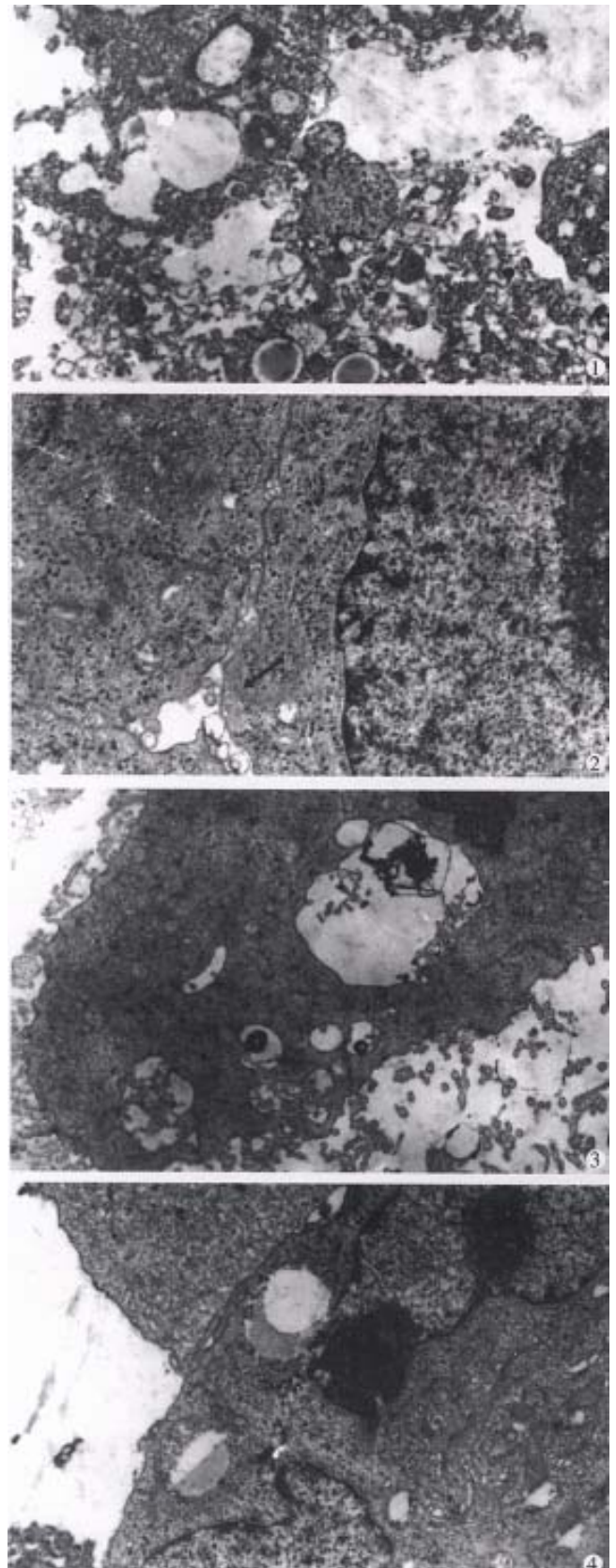


**Figure 3** Results of intratumoral injection of  $^{32}\text{P}$ -GMS demonstrated by electron microscopy: ①Necrosed tumor cells ( $\times$ 5000). ②Formation of bile duct-like structure among tumor cells (solid arrow) ( $\times$ 8 000). ③Plenty of microvilli on the surface of tumor cell ( $\times$ 7000). ④In control group, intratumoral injection of  $^{32}\text{P}$ -GMS showing heteromorphic tumor cell with cleavage of nucleus and scanty microvilli on surface ( $\times$ 7000).

**Table 3** Histological liver tissue parameter and estimated value of a absorbed dose in domestic pigs with hepatic arterial administration of <sup>32</sup>P-GMS

Animal serial No.	Sex	Route of medication	Time of death (wk)	<sup>32</sup> P-GMS (MPq·mg <sup>-1</sup> )		Weight (mg)	Tissue macrocosmic mean absorbed dose (Gy)
				Administered activity (MBq)	Cumulated activity (MBq)		
1	F	Right hepatic artery	1	0	0	300	
2	M	Left hepatic artery	2	0	0	260	
3	F	Hepatic artery proper	4	0	0	1353	
4	M	Hepatic artery proper	8	0	0	374	
5	F	Right hepatic artery	16	0	0	1000	
6	M	Right hepatic artery	1	925	266	313	48
7	F	Left hepatic artery	2	944	465	705	190
8	M	Hepatic artery proper	4	1070	825	375	104
9	F	Left hepatic artery	8	459	529	343	136
10	M	Right hepatic artery	16	461	459	349	61 <sup>△</sup>
11	F	Hepatic artery proper	16	0		0	
12	M	Hepatic artery proper	16	0		0	

<sup>△</sup>Calculated from the estimated liver weight of 1.5kg before medication.

**Serological manifestation** In warm sphere group, the lactic acid dehydrogenase level attained 2 folds to the upper limit of normal in human being at the beginning, and one week later it rose to 4-6 folds. It did not decline significantly to 3-4 folds until week 4, and then it continuously declined to the initial level at week 8. As for aspartate aminotransferase (AST) or  $\gamma$ -glutamyl transpeptidase ( $\gamma$ -GT) there was an elevation in different degree, but for total protein (TP) and total bilirubin (TB) no changes were observed. These items were neither found abnormal in the cold sphere group nor in blank control one. As for the markers of pig liver fibrosis, the basal level of HA was within normal human range (2 $\mu$ g/L-100 $\mu$ g/L), in the warm sphere group and rose to the peak and then declined to normal. While in the cold sphere one, it rose slightly at week 1, then restored gradually to normal. The initial level of hPCIII was 2 folds to the upper limit of normal (<120 $\mu$ g/L). Within two weeks of warm sphere administration it increased to 3 folds of the normal value and recovered to initial level within 8 weeks; for the cold sphere group, hPCIII value increased slightly at week 2, then returned to the initial level at week 4. There was no abnormality of above markers in the blank control group. In the dynamic studies of G-IV, C G and LN, no apparent alterations were found in any animal group.

**Light microscopy** In the portal area the debris of <sup>32</sup>P-GMS (Figure 4) was found. In the warm sphere group, some hepatocytes showed granulation and eosinophil granulocytes infiltration at week 2 and week 4; slight granulation of hepatocytes and some with fatty change were found at week 8; no apparent abnormalities were found at the week 16

and during the whole course in cold sphere and blank control groups. No apparent changes were seen in the lung, spleen, stomach and kidney of all the experimental animals.

**Electron microscopy (Figure 5)** By electron microscopic morphometric analysis, the  $N_{abn}$  and  $M_{var}$  of the hepatocytes are shown in Table 4. One to two weeks after internal irradiation, in the warm sphere group there were alterations in nuclei and mitochondria, dilatation of rough endoplasmic reticulum, local lytic injury in endothelial lining of sinusoid, and pale faint halo at the periphery of erythrocyte. No liver tissue abnormality was found in the cold sphere group. In warm sphere one at week 4 of internal irradiation, the hepatocytes still showed some abnormal features including decreased mitochondria, distended rough endoplasmic reticulum, detached ribosome, greatly increased lysosomes and myeloid bodies, bile canaliculi disrupted showing cholestasis, and vascular endothelium was prominently damaged. Eight weeks after irradiation, the injured hepatocytes decreased. There were plenty of organelles and glycogen particles in cytoplasm, intercellular junction among the hepatocytes showed normal configuration with regularly arranged microvilli, the matrix of mitochondria condensed, rough endoplasmic reticulum distended, and fat-storing cells of collagen fibers were prominently presented in the Disse's spaces; and endothelium of blood sinus was integrated and accompanied with neutrophil granulocytes infiltration. In the liver tissue of whole liver embolization with cold spheres the nuclei of hepatocytes remained normal, but the cytoplasm revealed the changes similar to those found 4 weeks-8 weeks after internal irradiation.

The liver tissue specimens taken at 16 week of internal irradiation demonstrated that most of the hepatocytes recovered almost to normal with abundant collagen fibers in the Disse's space, while those from cold sphere group were essentially normal. The liver tissue was morphologically normal in the whole course of blank control group.

**Table 4**  $N_{abn}$  and  $M_{var}$  of nucleated hepatocytes and their standard error ( $P \pm SE$ )

No. of week	Warm sphere group		Cold sphere group		Bland control	
	$N_{abn}$	$M_{var}$	$N_{abn}$	$M_{var}$	$N_{abn}$	$M_{var}$
1	60±4.09 <sup>a</sup>	80±4.00 <sup>a</sup>	9±2.86 <sup>c</sup>	5±2.18 <sup>c</sup>		
2	58±4.94 <sup>a</sup>	77±4.21 <sup>a</sup>	8±2.71 <sup>c</sup>	4±1.96 <sup>c</sup>		
4	38±4.85 <sup>b</sup>	60±4.90 <sup>b</sup>	5±2.18 <sup>c</sup>	6±2.37 <sup>c</sup>		
8	8±2.71 <sup>cd</sup>	12±3.25 <sup>ce</sup>	3±1.71 <sup>c</sup>	5±2.18 <sup>c</sup>		
16	4±1.96 <sup>cd</sup>	4±1.40 <sup>ce</sup>	2±1.40 <sup>c</sup>	2±1.96 <sup>c</sup>	2±1.40	2±1.40

Warm sphere group no statistical significance between week 1 and week 2,  $\chi^2=0.27$ , <sup>a</sup> $P<0.50$ . In warm sphere group comparison of week 1 and week 2 with week 4,  $\chi^2=6.70-9.68$ , <sup>b</sup> $P<0.01$  and with other groups,  $\chi^2=65.09-115.09$ , <sup>c</sup> $P<0.001$ .  $N_{abn}$  of week 8 compared with that of week 16,  $\chi^2=1.42$ , <sup>d</sup> $P<0.20$ .  $M_{var}$  of week 8 compared with that of week 16,  $\chi^2=7.68$ , <sup>e</sup> $P<0.01$ .

### Clinical application

**Therapeutic effectiveness (Table 5)** In groups A and B, most of the HCC patients with <sup>32</sup>P-GMS treatment revealed prominent symptomatic improvement, relief of pain in liver region, improvement of appetite, gain of body weight, decreased tumor-size and iodized oil condensed in the form of fragments or encapsulated cumulation on the film or CT (Figure 6). No collateral circulation around the tumor body was found after <sup>32</sup>P-GMS treatment, but in 5 cases of group A some secondary foci neighboring the primary foci which had been controlled, appeared within 2-3 months after therapy. no such problem was found in group B. In three cases of diffused type of HCC, the foci were not controlled effectively. Of the 79 cases of HCC, the post-treated tumor size as compared with their original sizes, was decreased more than 50%, 50%-25%, 25%-10% and less than 10% in 24 (30.37%) cases, 25 (31.64%), 22 (27.84%) and 8 (10.1%), respectively. After <sup>32</sup>P-GMS and TAE treatment in group B, 4 received surgical resections of tumor with fair results but the other 6 with decreased tumor size refused to be operated on. Twelve of 14 cases of metastatic hepatic carcinoma after regimen B and C treatment showed decrease in size of foci, giving an effective rate of 85.71%.

**Toxic or adverse effects** About 2-3 days after TAE treatment in group C, some patients experienced fever of 38.5 °C and had grade IV leukocytopenia, almost all patients had nausea, vomiting and upset

or pain in liver region. Serum ALT, ALP and bilirubin were slightly elevated, the markers of liver fibrosis HA and hPCIII revealed transient elevation, restored to the pretreatment level about half month later, C-IV, LN and CG did not show any fluctuation. no abnormalities were found in renal function and ECG. As compared with group C, the above features in group A patients were rare and mild, among them 7 cases had pre treatment WBC  $<2.0 \times 10^9/L$  and one patient with uremia under regimen A treatment did not present significant side effects or complications. In group B patients no grade III-IV gastrointestinal reaction and no grade IV leukocytopenia occurred after treatment (Table 6).

**Living quality and survival period** The median survival period of HCC patients in groups A and B was 585 days, in group C, 455 days. The 0.5, 1, 2 and 3 year survival rates in group A, B and C were 100%, 96.7%, 56.7%, 43.3%; 97.7%, 91.8%, 61.2%, 51.0% and 96.4%, 81.8%, 41.2%, 31.0%, respectively. The living quality of patients in groups A and B has improved prominently as evaluated by Karnofsky score, which rose from the basal level of 65.5 to 75.5, eventually to 80 in the recovery stage of some individual patients. A patient complicated with uremia maintained by hemodialysis survived up to 26 months after treatment, another patient committed suicide due to the cause unrelated to his illness. Two cases complicated with cancer cell embolism of portal vein survived merely 3.5 and 6.5 months and died from upper digestive tract bleeding and hepatorenal syndrome respectively.

### Prognostic factors affecting the survival rate

Multifactorial analysis revealed that the following prognostic factors may affect the survival rate: accumulation of <sup>32</sup>P-GMS in the tumor mass, parameters of hepatic fibrosis, the clinical types, size and its magnitude of decrease after treatment and whether intrahepatic or remote metastasis was present. The therapeutic effectiveness was not fully dependent upon the different histocytological types.

**Table 5** Comparison of effectiveness in different therapeutic groups

Grade of effectiveness	Group A	Group B (n)	Group C
>50%	9	15	4
50%-25%	7	18	5
25%-10%	9	13	5
<10%	5	3	4
Effective rate %	83.33	93.87	77.77

RIDIT analysis: A/C:  $\alpha \neq 0.05$ , no statistical difference between two groups. B/C:  $\alpha=0.05$ , significant difference between two groups.

**Table 6 Comparison of toxic hematological reaction in different groups**

Grading	Group A (n)			Group B (n)			Group C (n)		
	Hb	WBC	Plt	Hb	WBC	Plt	Hb	WBC	Plt
0	10	12	12	18	15	16	2	4	2
I	12	16	10	22	24	23	5	2	4
II	8	2	8	7	8	9	6	6	6
III				2	2	1	3	4	3
IV							2	2	3



**Figure4** Pig no.10 by intrahepatic artery instillation of  $^{32}\text{P}$ -GMS after 16wk, showing the glass fragments (solid arrow) in the portal area, the distorted venule in the lower part of the picture is the artifact due to compression of interlobular venule by the glass microsphere during preparing slide. HE stain  $\times 400$

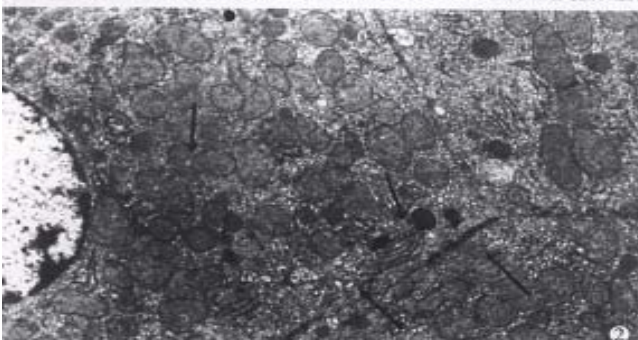


**Figure5** ①First week of internal irradiation irregularly distorted nuclei of hepatocytes, aggregation of heterochromatin at the periphery of nuclei, distension of perinuclear gap (solid arrow); decreased number of mitochondria in cytoplasm with heavy or light stained substance; dilatation of rough endoplasmic reticulum, depleted glycogen, and increased lysosomes and vacuoles.  $\times 10000$  ②16wk of internal irradiation: normal configuration of hepatocytes, plenty of plasma mitochondria with normal cristae (curved arrow), no distention of the rough endoplasmic reticulum pool (small arrow), nor mal cellular junction (solid arrow).  $\times 6000$

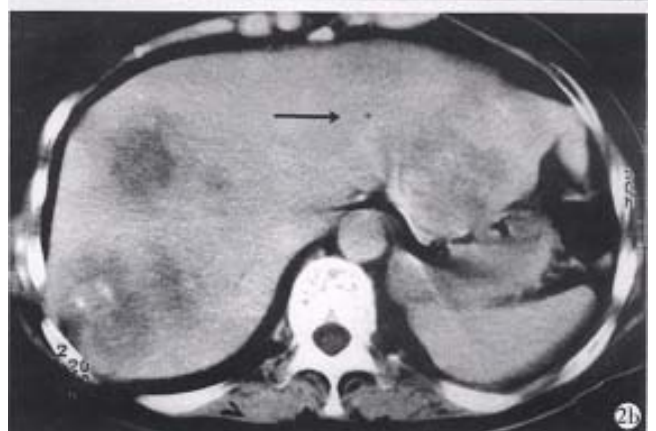
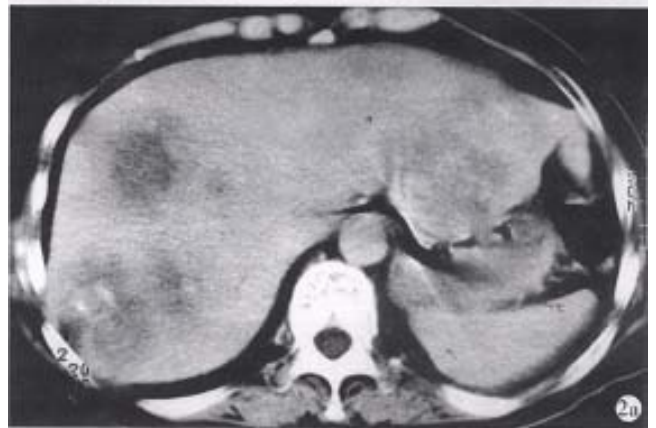


**Figure6** ①Case 1. Hepatic carcinoma, massive type, apparently decreased in size two months after  $^{32}\text{P}$ -GMS treatment (solid arrow). ②Case 2. Multiple metastatic hepatic tumor apparently decreased in size of left lobe focus after  $^{32}\text{P}$ -GMS treatment (solid arrow).

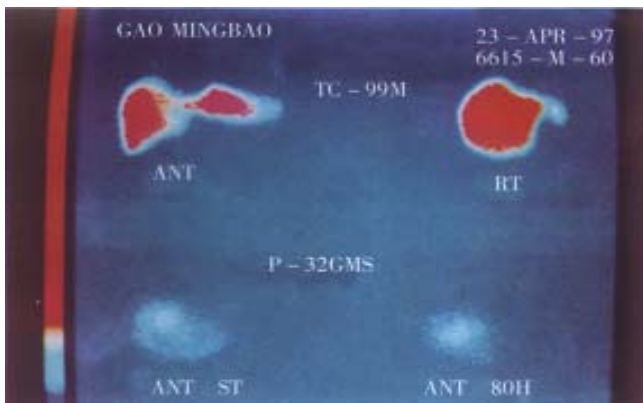


**Figure 7** SPECT imaging before and after  $^{32}\text{P}$ -GMS internal irradiation in patients with relapsed HCC (interlobular) after operation. Upper picture demonstrates interlobular colloidal image (anterio-posterior and light lateral position). Lower picture shows 80h after  $^{32}\text{P}$ -GMS treatment, most of  $^{32}\text{P}$ -GMS cumulated in the foci, no extrahepatic organ imaging was found.

## DISCUSSION

As the experiment demonstrated that the local internal irradiation of  $^{32}\text{P}$ -GMS surely had the cytotoxic effect on tumor cells and exerted a potent inhibitive effect on the growth of tumor even at the third day of medication. The  $\beta$ -ray generated from  $^{32}\text{P}$ -GMS exerted injurious effect on tumor tissue with very complicated mechanism: ①After the tumor cells absorbed the  $\alpha$ -ray energy, it directly affected the ionization and excitation of biological active macromolecules or broke its chemical bonds and destroyed the molecular structure. Since the active biological macromolecules were the main component of cell membrane, organelle and nucleus, defects in these structures apparently would reflect the impairment of their function. ②The indirect effect of  $\alpha$ -ray irradiation was to conduct ionization and irradiation of the water molecule in intracellular environment and to generate many kinds of free radicals and superoxides such as  $\text{O}_2$ ,  $\text{H}_2\text{O}_2$  etc. having very active chemical property with high oxidative toxicity. These irradiative products injured or destroyed the biological macromolecules<sup>[12]</sup>. ③ $\beta$ -ray acted on the cell DNA to induce the cell-death related gene expression, hence to accelerate the apoptosis of cancer cells<sup>[13]</sup>. When the cancer cells received massive dose of irradiation, the metabolic activity ceased immediately, the cell structure disrupted and lysed, resulting in cell death at metaphase; when the cancer cells received irradiation at a certain dosage, and fulfilled several times of multiplication, they would lose the ability of proliferation leading to proliferative death<sup>[14]</sup>. In addition,  $\beta$ -ray irradiation had the effect on occluding capillary vessels and inducing the hyperplasia of connective

tissue in tumor resulting in structural derangement and promotion of the injury and necrosis of tumor cells.

On the 14th day of local injection of  $^{32}\text{P}$ -GMS to the tumor, the tumor cell death rate was 43%-82% in different treatment groups, but 4% in control group. The anticancer effect of  $^{32}\text{P}$ -GMS was directly proportional to the dose administered. In a particular time period, the rate of tumor cell death exceeded its rate of proliferation, then the tumor decreased in size; on the contrary, the death rate of tumor cell did not exceed their rate of growth, the tumor growth might be somewhat inhibited in a certain extent too. In the specimens of different treatment groups, the tumor cells might exhibit as survived, denatured or necrosed (in early or typical changes). This reflected essentially the whole course of tumor cell progression from denaturing to cell death after irradiation. The ultrastructural changes demonstrated that under the effect of high-dose irradiation, the tumor tissues received a lethal radiation energy in a short period, resulting in nonexistence of tumor cells which had a high ability to synthesize endogenous protein. In subgroup I, two tumor masses ne crossed thoroughly the skin neighboring to one of them showing metaplasia. Whether this was the result of radiation injury evolving to malignant change and degeneration or not should be further investigated. Under the appropriate dose of irradiation (subgroup II and III), besides most of the tumor cells necrosed, the tendency of deriving to nearly normal histological picture evolved, such as plenty of microvilli on the cell surface, genesis of bile canaliculi-like structure, etc. These demonstrated that the  $^{32}\text{P}$ -GMS has the ability of killing the actively proliferative tumor cells and promoted the normalization of regenerative cells. These were similar to the effect of irradiation in trace amount which might stimulate and enhance the local metabolism of inflammatory tissues, accelerate the death of injured cells and promote the growth of normal tissue, but this was not found in control group. It is also observed that the synergistic effect of immunocytes, cytolytic phenomena and its inhibition on the dispersion of tumor cells were enhanced in the tumor cells or nearby tissues. It denoted that the anticancer effect of  $^{32}\text{P}$ -GMS was directly proportional to the time course of medication, based on the principle of after effect and cumulative effect of radioactive nuclide therapy. After intratumoral injection of  $^{32}\text{P}$ -GMS, it was not dispersed or displayed to the non-targeting tissue as confirmed by SPECT imaging. In comparison with intratumoral injection of ethyl alcohol<sup>[15]</sup> or acetic acid<sup>[16,17]</sup>,  $^{32}\text{P}$ -GMS needs no repeated injection, with minimal side reaction<sup>[18]</sup>.

Intratumoral injection of  $^{32}\text{P}$ -GMS was the best choice in treating the unresectable tumor or some metastasized lesion as well as those unsuitable for intra-arterial interventional therapy, it was also suitable for solid malignant tumors which could be reached anywhere on the human body.

We have got sufficient data from the dynamic study on the ultrastructural morphometric analysis of liver tissues taken from warm sphere, cold sphere and control groups. According to the injury of normal liver after internal irradiation and its repairing process, it was allocated into 4 periods: ① acute reactive period (within 2 weeks), ② subacute reactive period (2-4 weeks), ③ prerecovery period (4-8 weeks), ④ recovery period (8-16 weeks). In the acute period of warm sphere group, there was decreased proteosynthetic function and alteration of energy metabolism, decreased synthetic ability of ATP. The faint halo around the erythrocytes in the blood sinus as shown under electron microscopy probably was the super liquidized iodized oil. The disruption of sinusoidal endothelium was closely related to the route of medication. No apparent injury of hepatic tissue was found in the control group. This suggested that the serial changes in ultrastructure which was seen in the warm sphere group might be the result of radiation injury. The sinusoidal endothelium was most prominently disrupted. All these changes represented the synergistic action of internal irradiation and embolization. At the prerecovery period, the abnormal nuclei of hepatocytes were scarcely seen, but the cytoplasmic organelles recovered more slowly than the nuclei. Cell injury was resulting in increase in myeloid bodies in the cytoplasm, which indicated the liver tissue evolved into self-repairing stage. The hepatocytes appeared essentially normal in the recovery period. Electron microscopy revealed prominent collagen fibers in the Disse's space in some of the liver specimens, whether it indicated the tendency of early liver fibrosis or not should be further studied.

Recent evidences<sup>[19]</sup> showed the C-IV increases prominently in the early stage of liver fibrosis, LN is closely related to the genesis of liver fibrosis, and CG is the important marker for estimating the severity of biliary cirrhosis, but the serum C-IV, LN and CG all fell into the human normal range in the whole course of the experimental animals. Therefore, the presence of collagen fibers in the Disse's space was probably of transient local changes. The transient changes in HA value were similar to those of hPCIII, and the liver injury induced serum HA elevation was positively proportional to the severity of illness, and the serum hPCIII level was closely related to the extent of fibrosis. When the function of hepatocyte was

damaged, hPCIII might be released to circulation and often used as the guidance for selection of therapeutic medicine<sup>[20]</sup>. Therefore, the transient changes in domestic pig serum HA and hPCIII values were the impairment of liver function resulted from  $^{32}\text{P}$ -GMS administration. It was reported<sup>[21]</sup> that intra-hepatic arterial administration of cold spheres to the dosage equivalent to 12 folds of the human tolerable dose merely induced the clinically permissible intrahepatic changes and did not follow with portal fibrosis or hepatic cirrhosis after 90 days observation. The experiment demonstrated that the cold sphere slightly injured the hepatocytes, probably being the embolization of the nutritional artery rather than irradiation. In this experiment, through hepatic artery medication, no non-target organs developed in all of the domestic pigs. No prominent ultrastructural changes were found in the hepatic lobe during the whole course in the control animals. The experiment demonstrates that intrahepatic change of clinically permissible extent might be induced in the liver tissue of domestic pigs that received  $^{32}\text{P}$ -GMS in the macrocosmic average absorbed dosage of 48Gy-190Gy. These changes were reversible sublethal injury<sup>[14]</sup> and essentially recovered within 8 weeks. In the observation of 120 days there was no evidence of portal fibrosis. This is the evidence that superselective intrahepatic medication may yield a high energy region and without serious injury to the nearby non-medicated tissues or organs.

Hepatic artery embolization is the important measure in treating hepatic carcinoma<sup>[22,23]</sup>. Investigating an ideal embolizing agent is the substantial project in interventional therapy of tumor. The ideal internal radioactive nuclide should serve as a spotted source of radiation with high energy reserve and the carrier having high orientating rate, lasting longer in the target tissue, and the loaded nuclide was not easy in detaching or leaking to circulation.  $^{32}\text{P}$ -GMS, administrated through the hepatic artery, wedged in the terminals of this artery with its mixed iodized oil which was not absorbable could occlude the arterial capillary. In addition to the radiation obliteration of blood vessels induced by internal irradiation, the collateral circulation was not readily generated in the foci. All of the above mentioned advantages will benefit to boosting therapeutic efficiency. Therefore  $^{32}\text{P}$ -GMS is an appropriate internal radioactive embolizing agent with medium or long duration. It has been confirmed in the clinical investigation, the tumor in liver showed angiogenesis at the microcirculatory level and might trap microspheres 3-4 folds to that of normal liver tissue<sup>[24-26]</sup>. Instillation of therapeutic dose of radionuclide to the nutritional arteries of tumor, particularly condensed in the tumor tissue, may exert potent cytotoxic effect to

fulfill the purpose of therapy. It has been reported<sup>[27-29]</sup> that Yttrium-90-GMS ( $^{90}\text{Y}$ -GMS) used in intrahepatic arterial embolization got fair result, and the absorbed dosage attained 50Gy-100Gy in the tumor may have radical effectiveness<sup>[29]</sup>. Nevertheless  $^{90}\text{Y}$ -has the disadvantages of short half-life, inconvenienced in clinical application, and  $^{90}\text{Y}$ -GMS having smaller diameter, and higher hepato-pulmonary shunting index than that of  $^{32}\text{P}$ -GMS<sup>[30]</sup>. As reported that intratumoral injection of  $^{90}\text{Y}$ -GMS in 33 cases of hepatic carcinoma, the bremsstrahlung radiation conducted by SPECT showed 21.4% had development in lung, and 14.3% in intestine. In our study  $^{32}\text{P}$ -GMS in therapeutic dosage through superselective hepatic arterial regional instillation, particularly condensed in the tumor tissue including the central and peripheral portions, forming a high energy region and it is worth noting that extrahepatic development was not found (Figure 7). Therefore transhepatic artery administration of anticancer agent is the first choice in regional medication to treat hepatic tumor. If the hepatic artery is severely distorted or fails in catheterization, intraparenchymal injection of  $^{32}\text{P}$ -GMS should be considered instead.

The therapeutical results of TAE were inconsistent in different histocytological type of HCC<sup>[31]</sup>. The clear cell type was most sensitive, the small cell and poorly or undifferentiated type was moderately sensitive. Based on the radio-biology, cell sensitivity to nuclide beam depended upon the functional status of the cell proper. The cytotoxic effect and durability of  $^{32}\text{P}$ -GMS was superior to the other anticancer chemicals. The therapeutic results depended upon the clinical classification rather than histocytological types.

The results of clinical observation revealed that the clinical classification and the specific features of angiogram might be the basis for evaluating the therapeutical effectiveness and predicting the prognosis. The clinical materials suggested that the regimen B is superior to regimen A and C in the respect of decreasing tumor size and prolonging the survival period. The follow-up results demonstrated that the excellent effect was evolved in the cases with small tumors, plenty of blood supply, intact capsule and heavily aggregated  $^{32}\text{P}$ -GMS in the tumor as revealed by SPECT. Analysis of the clinical classification showed that in average survival time of the 3 clinical types of HCC solitary mass type was longer than the multiple and diffuse type. The patients with apparent decrease in AFP level were consistently accompanied with decrease in tumor size and necrosis in the tumor. In case of these features relapsed and elevation of AFP or complicated with intrahepatic or remote metastasis, all these would result in poor prognosis.

Strategy of therapy: for those hepatic

carcinoma with intact capsule and diameter below 6cm treated by the regimen A for 1 or 2 courses could get satisfactory result, and for those with occult metastatic foci, the secondary foci would be present besides the controlled original lesion several months later. It is of significance to use  $^{32}\text{P}$ -GMS and TAE in combination resulting in apparent synergetic effect (regimen B), which not only enhanced the anticancer and embolic effects but also lessened the side effects, and could completely cure the small liver cancer, eliminated the need of operation (Figure 8), diminished the number of medication with mild liver injury and low relapse rate. After undergoing regimen B treatment, some cases of unresectable tumor acquired the possibility of being resected (Figures 9, 10). The dosage of  $^{32}\text{P}$ -GMS should be decided by the specialists majoring in nuclear medicine and interventional therapy. The optimal schedule was to give two courses of medicine at an interval of 2 months, and as the tumor size decreased, the residual lesion should be resected as soon as possible in order to improve the survivability. There were few viable cancer cells in the 4 resected specimens on pathological examination after the regimen B treatment. Hepatic carcinoma readily invaded the portal vein with cancer cell emboli. It is apparent in such case that intrahepatic artery medication should be complemented with other measures as minimal invasive embolotherapy which will be an intelligent choice. For the metastatic abdominal lymph nodes intratumoral injection of  $^{32}\text{P}$ -colloids under the guidance of CT is also a helpful measure. It is emphasized that we should choose reasonable regimen, strict manipulation, superselective catheterization, well controlled speed in medication to avoid regurgitation of nuclide to the non-target blood vessel, and lessen the complication, particularly depending on the individualized situation. The hepatic arterio-venous fistula should be considered as the contraindication for medication via catheterization.

In conclusion,  $^{32}\text{P}$ -GMS which possesses the anticancer effect through interventional medication may block the blood supply to tumor and evenly distribute the highly concentrated anticancer medicines in the tumor to exert the radioactive cytotoxic effect with the advantage of low local radiation reaction and no apparent systemic toxic effect.  $^{32}\text{P}$ -GMS is an effective measure for the comprehensive treatment of hepatic cancer. Owing to the moderate half-life of  $^{32}\text{P}$ , the dosage of  $^{32}\text{P}$ -GMS required to attain the same absorbed radioactivity is approximately one-fourth or one-third of  $^{90}\text{Y}$ -GMS dosage<sup>[8]</sup>. Therefore it will satisfy the clinical requirement in reducing the risk of radiation to the handlers, simplifying the medical care and lowering the expenses. Thus, a hopeful prospective therapeutic weapon will be developed and popularized in the near future.

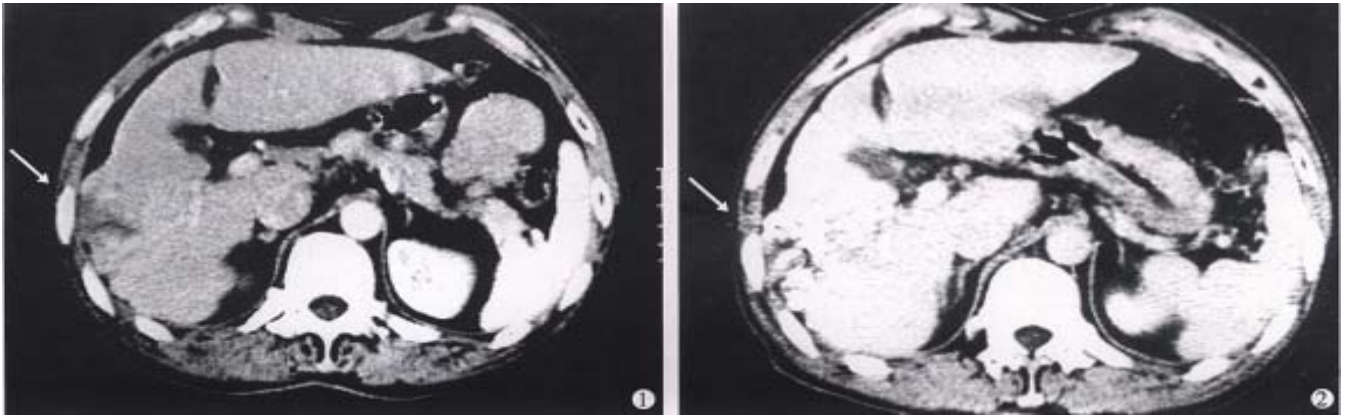


**Figure 8** Male, aged 60, hospital no.202929, clinical diagnosis: right lobe medium sized hepatic carcinoma (4cm×5cm), treated by regimen A and B with an interval of 2 months. AFP from 103 $\mu$ g/L restored to normal range, tumor size decreased >50%, CT: 1, on pre-treatment showing a low density region in right lobe (arrow), 2, on post-treatment iodized oil distributed in fragments or encapsulated forms (arrow). Body weight gained more than 5kg and no subjective symptoms on 36 months follow-up.

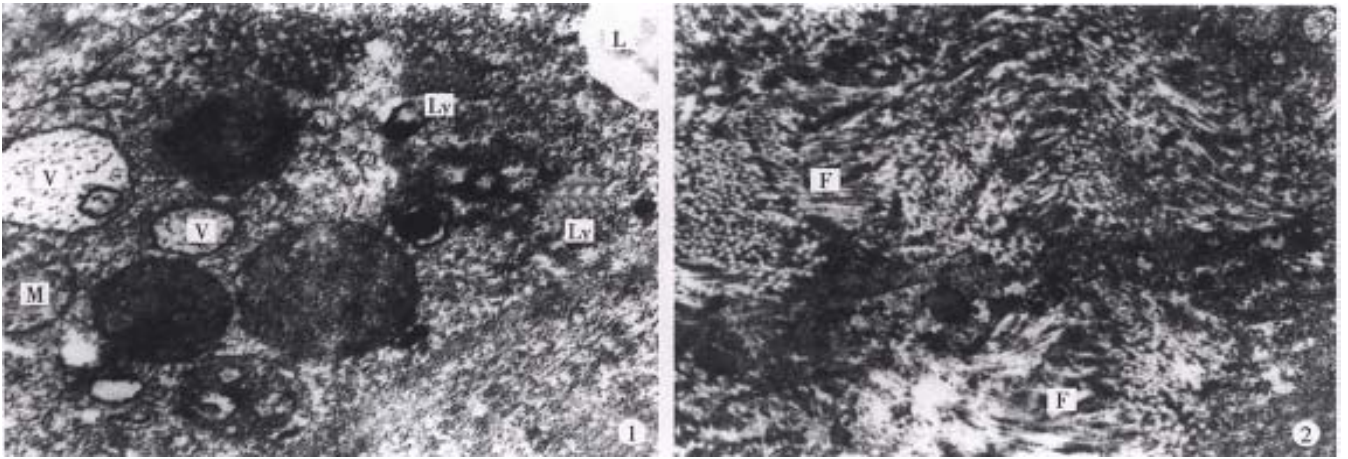


**Figure 9** Male, aged 55, hospital no.202295, clinical diagnosis: left lobe medium sized hepatic carcinoma (5cm×6cm) near the hepatic hilus, treated by TAE and regimen B, with interval of 2 months, and left hepatic lobectomy was performed 6 months later. The tumor (4cm×4cm) was with hard consistency, and encapsulated fibrotic degeneration. Most of the cancer cells showed necrosis under light microscopy. Some cancer cells in the cholecystic wall were alive (may be due to the blood supply from cholecystic artery). The electron microscopy showed: 1, cancer cells degenerated and necrotic; in cytoplasm some vacuolized mitochondria (M), irregular sized vacuoles (V) and lysosome (Ly) and lipid droplet (L) were seen. The rest structures were not clear ( $\times 30000$ ). 2, Prominent fibro-connective tissue hyperplasia (F) in the tumor tissue ( $\times 10000$ ) was found. Patient gained body weight and no subjective upset on follow up until 12 months after operation.

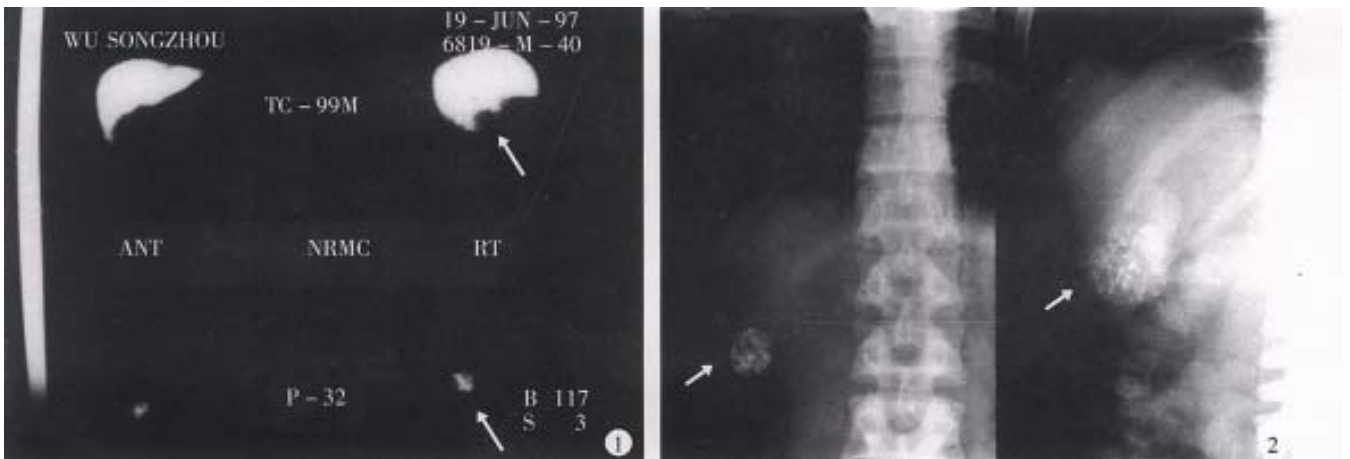


**Figure 10** Male, aged 41, hospital no.207089, clinical diagnosis: uremia, right hepatic small carcinoma (4cm×3cm), with AFP >400 $\mu$ g/L treated by regimen A for 2 courses with interval of 3 months, resulted in AFP restored to normal level and decreased tumor size over 50%. 1, Colloidal SPECT imaging showed the space occupying lesion in the right liver lobe (as shown by arrow). 2, Comparing the tumor size before and after treatment of plain film (as arrow shown), the patient died from renal failure 26 months after operation.

## REFERENCES

- 1 Tang YX, Jiang YD, Zhang Y, Li YJ, Nie Y, Zang H, Zhang XZ, Qiao WA, Lan FS. Observation on the therapeutic results of interventional irradiation in mid and late stage hepatic carcinoma. *Linchuang Yixue Yingxiang Zazhi*, 1997;8:224-225
- 2 Zhang YH, Wu YB. Advances of anticancer target preparation. *Zhongguo Yaoxue Zazhi*, 1992;27:389-393
- 3 Kobayashi H, Hidaka H, Kajiya Y, Tanoue P, Inoue H, Ikeda K, Nakajo M, Shinohara S. Treatment of hepatocellular carcinoma by transarterial injection of anticancer agents in iodized oil suspension or of radioactive iodized oil solution. *Acta Radiol Diag*, 1986;27:139-147
- 4 Herba MJ, Illescas FF, Thirlwell MP, Boos GJ, Rosenthal L, Atri M, Bret PM. Hepatic malignancies: improved treatment with intraarterial Y90. *Radiology*, 1988;169:311-314
- 5 Houle S, Yip TCK, Shepherd FA, Rotstein LE, Sniderman KW, Theis E, Cawthorn RH, Richmond Cox K. Hepatocellular carcinoma: pilot trial of treatment with Y 90 microspheres. *Radiology*, 1989;172:857-860
- 6 Sun WH, Zhang LZ, Li ML. Research on radiotherapy of 32 P glass microsphere. *Hedongli Gongcheng*, 1990;11:75-78
- 7 Loveinger R, Holt JG, Hine GJ. Internally administered radio isotopes. In: Hine GJ, Brownell GL, eds. Radiation Dosimetry. *New York: Academic Press*, 1956:801-873
- 8 Liu L, Sun WH, Wu FP, Han DQ, Teng GJ, Fan J. An experimental study of treatment of liver cancer by locally administration with phosphate 32 glass microspheres & estimation of tissue absorbed dose. *Nanjing Tiedao Yixueyuan Xuebao*, 1997;16:223-226
- 9 Bao JZ, Wang Y, Zhan RZ, Wu MC. Clonal analysis of a hepatocarcinoma cell line: an experimental model of tumor heterogeneity. *Zhongliu Fangzhi Yanjiu*, 1995;22:65-67
- 10 Common statistic form and method in the diagnosis and treatment of tumor. In standards for diagnosis and treatment of common malignant tumor in China, Section 9, edited by Dept Medical Administration, Ministry of Public Health, PRC. Beijing: Beijing Med Univ & China Union Med College Joint Press, 1991:10-15
- 11 Yang SQ, eds. Health statistics. 3rd edition. Beijing: The Public Health Press, 1993:43-181
- 12 Editorial board of practical oncology. Practical Oncology. Vol. 1. Beijing: People's Medical Press, 1997:406-413
- 13 Zheng DX. Advance in apoptosis research. *Zhonghua Binglixue Zazhi*, 1996;25:50-53
- 14 Liu XC, Han KC. Hygienic protection and safety transportation of radioactive materials. Beijing: *Zhongguo Tiedao Chubanshe*, 1990:55-66
- 15 Ohto M, Karasawa E, Tsuchiya Y, Kimura K, Saisho H, Ono T, Okuda K. Ultrasonically guided percutaneous contrast medium injection and aspiration biopsy using a real time puncture transducer. *Radiology*, 1980;136:171-176
- 16 Ohnishi K, Ohyama N, Ito S, Fujiwara K. Small hepatocellular carcinoma: treatment with US guided intratumoral injection of acetic acid. *Radiology*, 1994;193:747-752
- 17 Zhao YF, Wen QS, Jia ZS. Local acetic acid injection in the treatment of transplanted tumor in mice. *Shijie Huaren Xiaohua Zazhi*, 1999;7:43-45
- 18 Liu L, Fan J, Zhang J, Du MH, Wu FP, Teng GJ. Experimental treatment carcinoma in a mouse model by local injection of phosphorus 32 glass microspheres. *J Vasc Interv Rad*, 1998;9:166
- 19 Ueno T, Inuzuka S, Torimura T, Oohira H, Ko H, Obata K, Sata M, Yoshida H, Tanikawa K. Significance of serum type IV collagen levels in various liver diseases. *Scand J Gastroenterol*, 1992;27:513-520
- 20 Axel MG, Wolfgang T, Anne N, Karl Heinz PK. Serum concentrations of laminin and aminoterminal propeptide of type III procollagen in relation to the portal venous pressure of fibrotic liver diseases. *Clin Chim*, 1986;161:249-258
- 21 Wollner I, Knutsen C, Smith P, Prieskorn D, Chrisp C, Andrews J, Juni J, Warber S, Klevering J, Crudup J, Ensminger W. Effects of hepatic arterial yttrium-90 glass microspheres in dogs. *Cancer*, 1988;61:1336-1344
- 22 Wang DZ, Sun WH, Zheng GY, Li ML, Wen YM. A study about the anticancer effect and the clinical application of the phosphate 32 glass microspheres (P32 GMS) by local arterial infusion. I. The ultrastructural study after internal radiation of P 32GMS in cancer cells. *Huaxi Kouqiang Yixue Zazhi*, 1991;9:7-10
- 23 Chen XL, Wu YT, Yan LN, Li L, Tan TZ, Sun WH, Li ML, Jia QB, Du JP, Shen WL. Treatment of liver cancer with 32P glass microsphere-an experimental study. *Puwai Jichuyulinchuang Zazhi*, 1996;3:68-70
- 24 Blanchard RJ, Grotenhuis I, Lafave JW, Perry JF. Blood supply to hepatic V2 carcinoma implants as measured by radioactive microspheres. *Proc Soc Exp Biol Med*, 1965;118:465-468
- 25 Sundqvist K, Hafstrom I, Perrson B. Measurements of total and regional blood flow and organ blood flow using Tc-99m labeled microspheres. *Eur Surg Res*, 1978;10:433-443
- 26 Gyves JW, Ziessman HA, Ensminger WD, Thrall JH, Niederhuber JE, Keyes JW, Walker S. Definition of hepatic tumor microcirculation by single photon emission computerized tomography (SPECT). *J Nuc Med*, 1984;25:972-977
- 27 Yan ZP, Lin G, Zhao HY, Dong YH. An experimental study and clinical pilot trials on yttrium 90 glass microspheres through the hepatic artery for treatment of primary liver cancer. *Cancer*, 1993;72:3210-3215
- 28 Andrews JC, Walker SC, Ackermann RJ, Cotton LA, Ensminger WD, Shapiro B. Hepatic radioembolization with yttrium-90 containing glass microspheres: preliminary results and clinical follow-up. *J Nucl Med*, 1994;35:1637-1644
- 29 Shepherd FA, Rotstein LE, Houle S, Yip TCK, Paul K, Sniderman KW. A phase I dose escalation trial of yttrium-90 microspheres in the treatment of primary hepatocellular carcinoma. *Cancer*, 1992;70:2250-2254
- 30 Tian JH, Xu BX, Zhang JM, Dong BW, Liang P, Wang XD. Ultrasound guided internal radiotherapy using yttrium 90 glass microspheres for liver malignancies. *J Nucl Med*, 1996;37:958-963
- 31 Wang YP, Zhang JS, Gao YA. Therapeutic efficacy of transcatheter arterial embolization of primary hepatocellular carcinoma: discrepancy in different histopathological types of HCC. *Zhonghua Fangshexue Zazhi*, 1997;31:586-588

Edited by WU Xie-Ning and MA Jing-Yun  
 Proofread by MIAO Qi-Hong